Feed-forward mechanism of converting biochemical cooperativity to mitotic processes at the kinetochore plate

Jung-Eun Park[a], Raymond L. Erikson[b,1], and Kyung S. Lee[a,1]

[a]Laboratory of Metabolism, Center for Cancer Research, National Cancer Institute, National Institutes of Health, Bethesda, MD 20892; and [b]Department of Molecular and Cellular Biology, Harvard University, Cambridge, MA 02138

Contributed by Raymond L. Erikson, March 11, 2011 (sent for review December 10, 2010)

The feed-forward mechanism is observed in some of the intracellular events, such as metabolic and transcriptional regulatory networks, but not in dynamic mitotic processes. Mammalian polo-like kinase 1 (Plk1) rapidly accumulates at centrosomes and kinetochores as cells enter mitosis. Plk1 function is spatially regulated through the targeting activity of the polo-box domain (PBD) that binds to a phosphoepitope generated by either cyclin dependent kinase 1 (Cdk1) (non-self-priming) or Plk1 itself (self-priming). "Non-self-priming and binding" is thought to ensure the orderly execution of cell cycle events. The physiological significance of the "self-priming and binding" is unknown. Using a pair of ELISA, here we demonstrated that mutations of the self-priming site of a kinetochore component, PBIP1/MLF1IP/KLIP1/CENP-50/CENP-U (PBIP1), to a Cdk1-dependent non-self-priming site abolished product-activated cooperativity in the formation of the Plk1–PBIP1 complex. Both PBD-dependent "two-dimensional" interaction with surface-restricted PBIP1 and subsequent phosphorylation of PBIP1 by anchored Plk1 were crucial to cooperatively generate the Plk1–PBIP1 complex. Highlighting the importance of this mechanism, failure in this process resulted in improper Plk1 recruitment to kinetochores, mitotic arrest, chromosome missegregation, and apoptosis. Thus, Plk1 PBD-dependent biochemical cooperativity is tightly coupled to mitotic events at the kinetochore plate through a product-activated, feed-forward mechanism. Given the critical role of self-priming and binding in the recruitment of Plk1 to surface-confined structures, such as centrosomes, kinetochores, and midbody, we propose that the observed feed-forward mechanism serves as a fundamental biochemical process that ensures dynamic nature of Plk1 localization to and delocalization from these subcellular locations.

Throughout evolution, various mechanisms have been developed to efficiently respond to extracellular stimuli that elicit a wide spectrum of cellular processes, including proliferation, differentiation, or apoptosis. Studies on diverse signal transduction pathways revealed that extracellular signals are frequently amplified at intracellular rate-limiting steps through a positive-feedback loop of activating an upstream activator(s) by a downstream component(s). Unlike these signaling pathways, dynamic intracellular processes, such as mitotic events, require concerted processes of both biochemical and cellular events. However, little is known about whether, and if so how, intracellular biochemical steps are amplified and converted into specific cellular events to efficiently cope with an acute physiological need at a certain stage of the cell cycle.

Mammalian polo-like kinase 1 (Plk1) is a member of the conserved Polo subfamily of Ser/Thr protein kinases that is essential for bipolar spindle formation and mitotic progression (1–4). Plk1 localizes to the centrosomes, kinetochores, and midbody in a manner that requires the function of the polo-box domain (PBD) in the C-terminal noncatalytic region (5–7). PBD forms a conserved phospho-Ser/Thr-binding module (8, 9) and binds to a phosphoepitope generated either by cyclin dependent kinase 1 (Cdk1) or other Pro-directed kinases (called non-self-priming and binding) or by Plk1 itself (called self-priming and binding) (10). However, whether these two PBD-binding mechanisms are physiologically distinct processes is not known.

We previously demonstrated that Plk1 phosphorylates a kinetochore protein called PBIP1/MLF1IP/KLIP1/CENP-50/CENP-U (hereafter referred to as PBIP1) at T78, and this priming step is a prerequisite for subsequent interaction between Plk1 PBD and the T78 motif of PBIP1 (11, 12). Loss of this interaction results in improper recruitment of Plk1 to kinetochores, mitotic arrest, abnormal chromosome segregation, and apoptosis (11, 13–15), suggesting that normal recruitment of Plk1 to kinetochores via self-priming and binding is crucial for proper M-phase progression. Distinctively from other self-priming and binding targets, such as PRC1 (16), HsCYK4 (17), and MKLP2 (18), both Plk1 and Cdk1 activities are present at PBIP1-loaded kinetochores, thus providing an ideal situation to comparatively investigate the physiological significance of self- versus non-self-priming. Here, we demonstrate that, unlike the positive-feedback loop that simply potentiates the activity of upstream kinase(s), self-priming and binding utilizes a Plk1 PBD-dependent biochemical cooperativity to rapidly generate additional PBD-binding sites, thereby accelerating its own recruitment to kinetochores and triggering Plk1-dependent mitotic events at this location. Thus, self-priming and binding is a product-activated, feed-forward mechanism that drives a given cellular event in an autonomous fashion. Highlighting the importance of this mechanism, failure in this process results in mitotic arrest, chromosome missegregation, and aneuploidy, a hallmark of cancer.

Results

Specificity of in Vivo Phosphorylation of PBIP1 and PBIP1-Cdk. To investigate the physiological significance of the self-priming and binding mode of the Plk1–PBIP1 interaction, we first generated a Cdk (mostly, Cdk1/Cyclin B1 in mitotic cells)-phosphorylable PBIP1-cdk mutant by mutating the Plk1-specific T78 motif of PBIP1 to a Cdk1 phosphorylation motif (Fig. 1*A*), as previously described (19, 20). Testing of GST-fused PBIP1 or PBIP1-cdk peptide spanning the T78 region (referred to hereafter as PBIPtide or PBIPtide-cdk, respectively) revealed that Plk1 specifically phosphorylates PBIPtide, whereas Cdk1 specifically phosphorylates PBIPtide-cdk in vitro (Fig. S1 *A* and *B*).

Then, we generated HeLa cells expressing EGFP-fused PBIPtide or PBIPtide-cdk to test the specificity of these EGFP-PBIPtides in vivo. As expected, they did not exhibit any distinguishable subcellular localization due to the lack of a localization signature within the PBIPtides (Fig. S1*C*). In early interphase,

Author contributions: J.-E.P. and K.S.L. designed research; J.-E.P. performed research; R.L.E. and K.S.L. analyzed data; and J.-E.P. and K.S.L. wrote the paper.

The authors declare no conflict of interest.

[1]To whom correspondence may be addressed. E-mail: erikson@mcb.harvard.edu or kyunglee@mail.nih.gov.

This article contains supporting information online at www.pnas.org/lookup/suppl/doi:10.1073/pnas.1102020108/-/DCSupplemental.

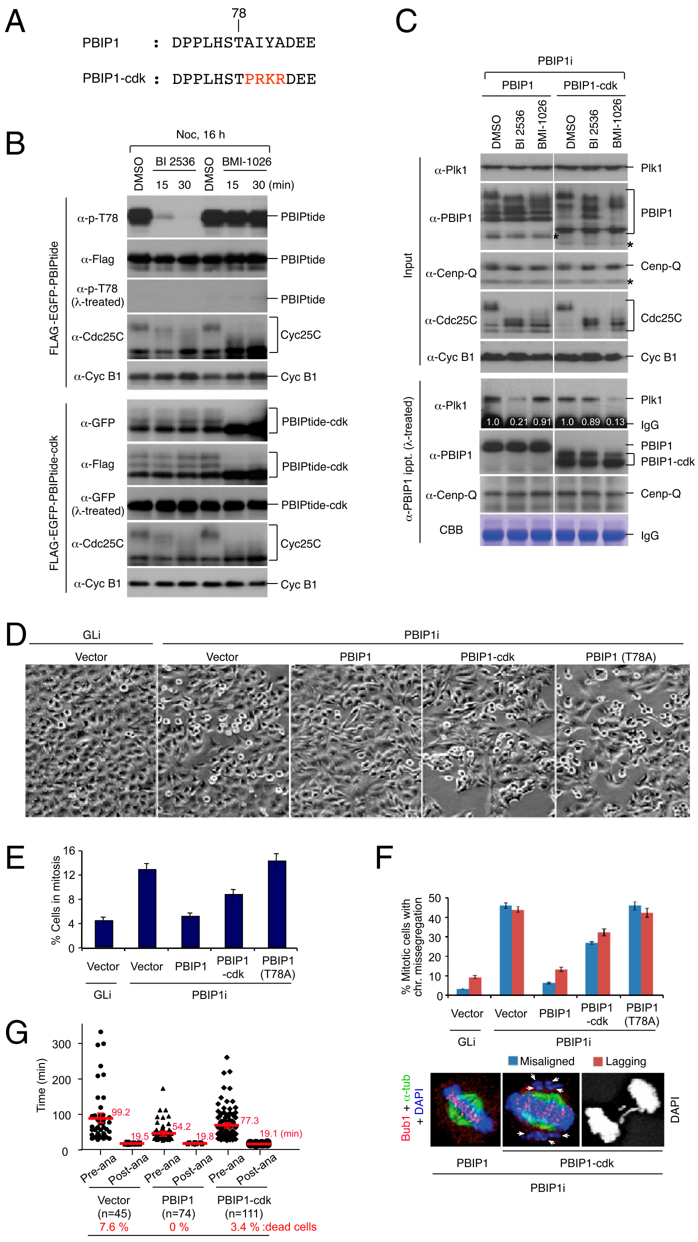

Fig. 1. Mitotic defects associated with the cells expressing the PBIP1-cdk mutant, but not the respective PBIP1 WT. (*A*) The indicated Pro-directed mutations (red) were introduced into PBIP1 to generate the PBIP1-cdk mutant. The T78 residue of PBIP1 is marked. (*B*) HeLa cells stably expressing EGFP-PBIPtide or EGFP-PBIPtide-cdk were arrested with nocodazole for 16 h, treated with either control DMSO, BI 2536, or BMI-1026, and then immunoblotted. Because anti-p-T78 antibody failed to detect the T78 phosphorylated PBIPtide-cdk, anti-GFP antibody was used to reveal λ phosphatase-sensitive modification of the protein. PBIPtide and PBIPtide-cdk, PBIP1- and PBIP1-cdk-derived peptides, respectively, bearing the T78 motif. As expected, BMI-1026 rapidly diminishes the level of the phosphorylated and slow-migrating Cdc25C, whereas BI 2536 decreases it only weakly. The same levels of Cyclin B1 indicate an unaltered cell cycle by the inhibitor treatment. (*C*) HeLa cells expressing RNAi-insensitive full-length PBIP1 or PBIP1-cdk were silenced for endogenous PBIP1 (PBIP1i), and arrested with nocodazole for 16 h. Prior to harvest, cells were treated with control DMSO or BI 2536 for 2 h, or BMI-1026 for 30 min to avoid precocious mitotic exit. After immunoprecipitation (ippt.), samples were treated with λ phosphatase and then immunoblotted. Numbers indicate relative efficiencies of Plk1 coimmunoprecipitation; asterisks, cross-reacting proteins. (*D*–*F*) HeLa cells stably expressing control vector or the indicated RNAi-insensitive PBIP1 forms were depleted of endogenous PBIP1 and released synchronously from a G1/S block. Samples harvested at various time points after release were immunoblotted to monitor cell cycle progression (see Fig. S2*A*). The cells released for 21 h were photographed (*D*) and quantified to determine mitotic indices (*E*). The cells from the 9-, 10.5-, and 12-h time points after release were either coimmunostained with the indicated antibodies after 10-min cold treatment (*Left*) or stained with DAPI alone (*Right*). Aberrant mitotic cells were quantified among the mitotic population (*F*). Arrows indicate misaligned (*Center*) and lagging chromosomes (*Right*). Error bars indicate standard deviation. (*G*) The cells in *D* were infected with lentivirus expressing EGFP-histone H2B and subjected to time-lapse microscopy 7 h after release from a G1/S block. The lengths of time spent for pre- and postanaphase progression were quantified. Numbers indicate the averages of time length with standard error of the mean. Representative still images and videos of cells obtained from the time lapse are available as Fig. S2 *D*–*G* and Movies S1–S4.

both PBIPtides did not appear to be significantly phosphorylated (Fig. S1*D*). In mitotic cells, however, inhibition of Plk1 activity by BI 2536 (21) acutely diminished the level of the phospho-T78 (p-T78) epitope in PBIPtide, whereas inhibition of Cdk1 activity by BMI-1026 (22) precipitously reduced the level of λ phosphatase-sensitive PBIPtide-cdk modification (Fig. 1*B*; note that because anti-p-T78 antibody failed to detect the p-T78 epitope of the PBIPtide-cdk mutant, we examined the total phosphorylation level of this protein). Furthermore, treatment of cells with BI 2536 or BMI-1026 specifically impaired the ability of Plk1 to interact with the full-length PBIP1 or PBIP1-cdk, respectively (Fig. 1*C*), indicating that the interaction is specifically regulated by the in vivo phosphorylation activity of Plk1 or Cdk1. Notably, although the cdk mutations induced a shift in gel mobility, PBIP1-cdk interacted with Plk1 normally and formed a complex with a kinetochore protein, CENP-Q, efficiently (Fig. 1*C*, compare lane 4 with lane 1), suggesting that these mutations do not alter other PBIP1 functions.

Mitotic Defects Associated with the PBIP-Cdk Mutation. Next, we generated HeLa cells expressing either control vector or the indicated shRNA-insensitive PBIP1 constructs, depleted of control luciferase (GLi) or endogenous PBIP1 (PBIP1i), and then released from a double thymidine block (G1/S) to monitor cell cycle progression. Twenty-one hours after release, both GLi cells expressing control vector and PBIP1i cells expressing WT PBIP1 exhibited only a low level of mitotic cells (Fig. 1 *D* and *E*). Under these conditions, PBIP1i cells expressing PBIP1-cdk showed a significantly increased (8.5%) mitotic index, although less than the cells expressing control vector or the dominant-negative PBIP1 (T78A) mutant (11) (Fig. 1 *D* and *E*). In line with these observations, both PBIP1-cdk and PBIP1 (T78A), but not PBIP1, cells exhibited a sustained level of slow-migrating, hyperphosphorylated Cdc25C (Fig. S2 *A* and *B*), suggesting a defect in proper M-phase progression.

Subsequent immunostaining analyses revealed that the PBIP1-cdk and PBIP1 (T78A) cells exhibited a large fraction of mitotic cells with misaligned or lagging chromosomes (Fig. 1*F*). These cells also displayed a significant level of interphase micronucleated morphology (Fig. S2*C*) generated presumably after bypassing the mitotic block imposed by misaligned chromosomes. In all cases, the PBIP1-cdk cells were less defective than the control vector- or PBIP1 (T78A)-expressing cells, suggesting that the PBIP1-cdk mutations impair, but do not annihilate, the function of PBIP1. Consistent with these observations, the PBIP1-cdk mutant exhibited a moderate level of preanaphase delay (an average of 77.3 min) when compared with the cells expressing either the control vector (an average of 99.2 min) or PBIP1 (an average of 54.2 min) (Fig. 1*G*; see also Fig. S2 *D–G* and Movies S1–S4).

Improper Recruitment of Plk1 to the PBIP1-Cdk-Loaded Kinetochores. After depleting endogenous PBIP1, we next examined the subcellular localization patterns of exogenously expressed PBIP1 and PBIP1-cdk. Reminiscent of endogenous PBIP1 (11), both PBIP1 and PBIP1-cdk strongly localized to interphase centromeres and moderately to mitotic kinetochores (Fig. S3 *A* and *B*). Reflecting a low abundance and activity of interphase Plk1 (23, 24), the efficiency of Plk1 recruitment to the PBIP1 or PBIP1-cdk-localized, interphase centromeres was low (Fig. 2*A*). During mitosis, Plk1 was efficiently recruited to the PBIP1-loaded prometaphase and metaphase kinetochores. In contrast, the efficiency of Plk1 recruitment to the PBIP1-cdk-loaded kinetochores was significantly decreased (Fig. 2*A*; see also Fig. S3 *A* and *B*), even though the kinetochore-bound PBIP1-cdk was slightly more abundant than PBIP1 (Fig. S3*C*). The less pronounced defect in Plk1 recruitment to the PBIP1-cdk-loaded prometaphase kinetochores in Fig. 2*A* could be due to the presence of other Plk1 PBD-binding kinetochore components, such as Bub1, BubR1, or INCENP (25–27) at this stage. Notably, Cyclin B1 fluorescent signals were detected at kinetochores as well as along mitotic spindles in preanaphase cells (Fig. 2*B* and Fig. S4 *A–C*), suggesting that the impaired recruitment of Plk1 to the PBIP1-cdk-loaded kinetochores is not because of the unavailability of Cdk1/Cyclin B1 activity at this location. Moreover, both Cyclin B1 and Plk1 signals were manifest at the kinetochores of misaligned chromosomes in taxol-treated cells (Fig. 2*C*), supporting the previous observation that Plk1 and Cyclin B1 are enriched at the kinetochores of misaligned chromosomes (28, 29). Thus, the suboptimal level of Plk1 recruited to the PBIP1-cdk-loaded kinetochores is likely because of less efficient formation of the Plk1–PBIP1-cdk complex than that of the Plk1–PBIP1 complex. Consistent with this view, PBIP1 sharply bound to Plk1 9 or 10.5 h after G1/S release (Fig. 2*D*). In contrast, PBIP1-cdk interacted with Plk1 approximately fourfold less efficiently, but formed the complex as early as 3 h after the release (Fig. 2*D*), likely as a result of the presence of G1 and S-phase Cdk activities.

Requirement of PBD-Dependent "Anchored" Reaction and "Two-Dimensional" Surface Interaction for the Product-Activated, Feed-Forward Phosphorylation of PBIPtide by Plk1. To understand the underlying mechanism of how PBIP1 recruited Plk1 more efficiently than PBIP1-cdk, we comparatively investigated the biochemical basis of Plk1-dependent PBIP1 phosphorylation with that of Cdk1-dependent PBIP1-cdk phosphorylation. To this end, we used a pair of ELISA-based kinase assays that are designed to quantify the level of intracellular Plk1 bound to the p-T78 motif of either Plk1-phosphorylated PBIPtide or Cdk1-phosphorylated PBIPtide-cdk (Fig. 3*A*; see *Materials and Methods* for details). A PBIPtide-cdk-based ELISA was developed by modifying the previously reported PBIPtide-based ELISA (30). Total mitotic lysates were used as a source of Plk1 and Cdk1 activities to reflect the in vivo circumstance of Plk1/Cdk1-dependent reactions. Under these conditions, the addition of BI 2536 (to inhibit Plk1) or BMI-1026 (to inhibit Cdk1) into the total mitotic lysates specifically diminished the level of Plk1 bound to PBIPtide or PBIPtide-cdk, respectively (Fig. 3*B*), thus demonstrating the specificity of the assays.

Next, we investigated the mode of Plk1- or Cdk1-dependent phosphorylation onto PBIPtide or PBIPtide-cdk, respectively,

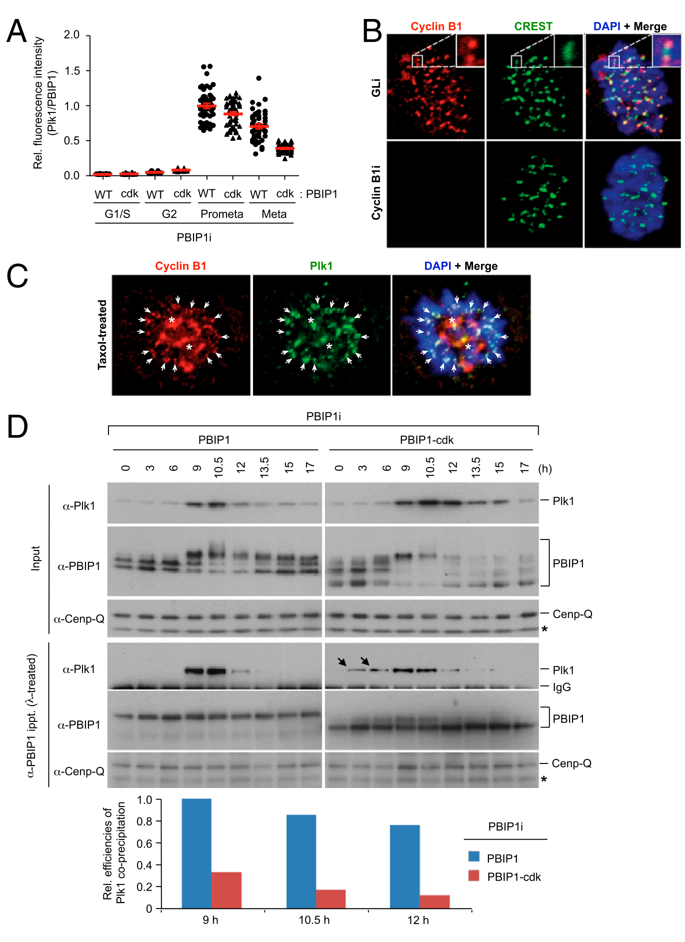

Fig. 2. PBIP1, but not PBIP1-cdk, properly recruits Plk1 to kinetochores via the efficient formation of the Plk1–PBIP1 complex during mitosis. (*A*) HeLa cells stably expressing either PBIP1 or PBIP1-cdk were depleted of endogenous PBIP1 and immunostained to determine the relative efficiency of Plk1 recruitment to the PBIP1-loaded kinetochores. Red bars indicate the averages of recruited PBIP1 or PBIP1-cdk intensities with standard error of the mean. WT, PBIP1; cdk, PBIP1-cdk. Note that the level of relative Plk1 signals at prometaphase kinetochores is greater than that at metaphase kinetochores, likely because of the presence of PBIP1-independent Plk1 recruitment at this stage. A very low efficiency of Plk1 recruitment to PBIP1-loaded interphase centromeres is in part due to a low abundance of interphase Plk1. (*B*) HeLa cells silenced for either control luciferase (GLi) or Cyclin B1 (Cyclin B1i) were treated with nocodazole to eliminate spindle-associated Cyclin B1 signals, and then coimmunostained with the indicated antibodies. The enlarged image shows a pair of Cyclin B1 signals flanking the CREST signal. (*C*) HeLa cells released for 11 h from a G1/S block were treated with 30 nM taxol for 2 h and then immunostained. Note that colocalized Cyclin B1 and Plk1 signals were detected at kinetochores (arrows) and centrosomes (asterisks). (*D*) Cells in *A* were arrested by double thymidine block and then released. Samples were immunoprecipitated (ippt.), treated with λ phosphatase, and then immunoblotted. To determine the relative efficiencies of the interaction between Plk1 and PBIP1 or PBIP1-cdk, the relative levels of coimmunoprecipitated Plk1 in the 9-, 10.5-, and 12-h samples were first determined by comparing them with their respective Plk1 inputs, which were then normalized by the amount of PBIP1 or PBIP1-cdk ligand immunoprecipitated. As a result of a mitotic arrest in the PBIP1-cdk cells, the level of Plk1 sustains for a long period of time. Likely due to the presence of G1 and S-phase Cdk activities, a low level of Plk1 coprecipitates in the 3- and 6-h PBIP1-cdk samples (arrows).

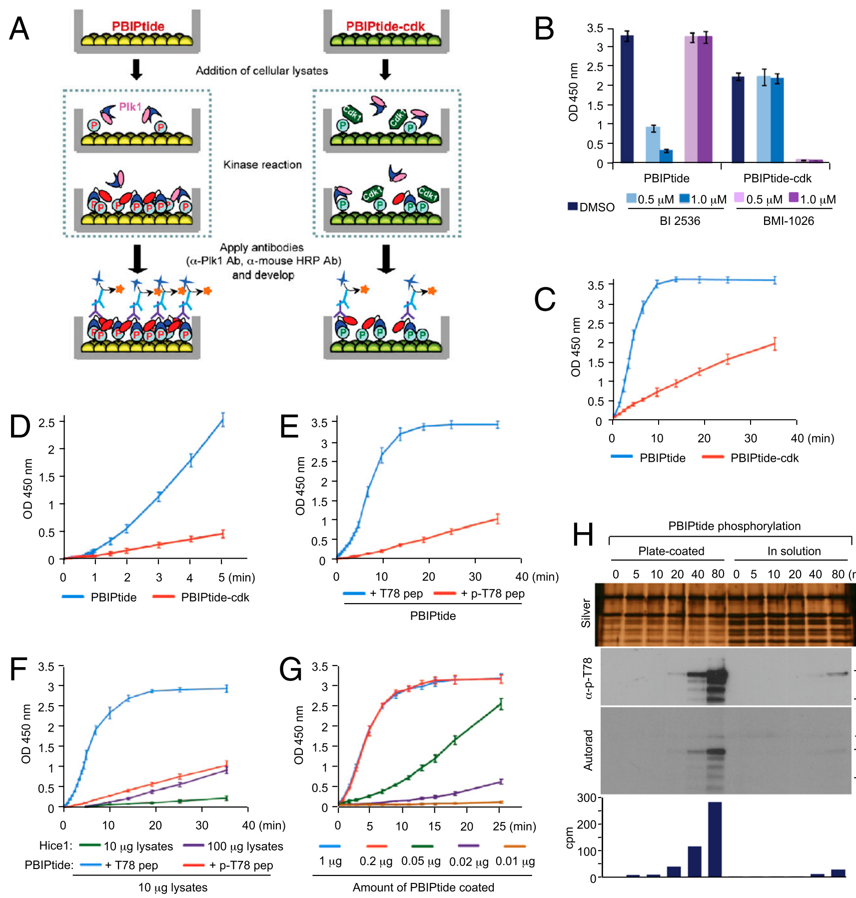

Fig. 3. Cooperative phosphorylation of PBIPtide, but not the PBIPtide-cdk mutant, by PBD-dependent Plk1 activity. (*A*) Scheme illustrating the experimental procedures of ELISA-based Plk1 or Cdk1 kinase assays using PBIPtide or PBIPtide-cdk, respectively, as substrates. ELISA wells coated with PBIPtide or PBIPtide-cdk were incubated with mitotic HeLa lysates for a specified length of time. Subsequently, the level of Plk1 bound to the p-T78 epitope of PBIPtide or PBIPtide-cdk was quantified by using anti-Plk1 and anti-mouse HRP antibodies. Pink and red oval, unactivated and activated Plk1 kinase domain, respectively; blue crescent, PBD. (*B*) Mitotic HeLa lysates were prepared and treated with control DMSO, BI 2536, or BMI-1026 for 30 min. The resulting lysates (100 μg/well) were incubated with the PBIPtide or PBIPtide-cdk ELISA plate for 30 min. Bars, standard deviation. (*C* and *D*) ELISA was performed as described in *A*. After terminating the reactions at the indicated time points, the level of bound Plk1 was quantified. Bars, standard deviation. (*E*–*G*) ELISA was performed similarly as in *C* and *D* with the following modifications. (*E*) ELISA was carried out with mitotic HeLa lysates mixed with either 13-mer non-phospho-T78 or corresponding p-T78 peptide, and the level of the p-T78 epitope generated on PBIPtide was quantified with anti-p-T78 antibody. (*F*) GST-Hice1 was used as a PBD-binding site-deficient Plk1 substrate. The level of Plk1-dependent Hice1 phosphorylation at S151 was quantified and compared with that of Plk1-dependent PBIPtide phosphorylation at T78. (*G*) ELISA was carried out using various levels of PBIPtide immobilized on the wells as substrate. Bars, standard deviation. (*H*) In vitro kinase assay was performed using PBIPtide, either immobilized on the well (plate-coated) or provided in solution, and soluble His-Plk1 (10 ng/reaction). After terminating the reactions, samples were retrieved from the ELISA plate and analyzed.

as a function of time. Interestingly, the level of Plk1 bound to the Plk1-generated (i.e., self-primed) p-T78 PBIPtide increased rapidly over time and exhibited sigmoidal kinetics (Fig. 3*C*; see also Fig. S5*A*), suggesting that Plk1 phosphorylates the T78 motif of PBIPtide in a cooperative manner. In stark contrast, the level of Plk1 bound to the Cdk1-generated p-T78 PBIPtide-cdk increased in a linear fashion (Fig. 3*C*). In a second reaction with a shorter timescale, a cooperativity was clearly observed with the Plk1-dependent PBIPtide phosphorylation, but not with the Cdk1-dependent PBIPtide-cdk phosphorylation (Fig. 3*D*; see also Fig. S5*B*). Both of these reactions exhibited similar initial rates of reactions (Fig. S5*B*, graphs). Strikingly, provision of a PBD-binding p-T78 peptide, but not the corresponding non-phospho-T78 peptide, completely eliminated the cooperativity (Fig. 3*E*; see also Fig. S5*C*). In addition, Plk1-dependent phosphorylation onto a PBD-binding site-deficient GST-Hice1, an Augmin complex subunit, increased linearly over time (Fig. 3*F*; also see Fig. S5*D*). Hence, PBD-dependent anchoring onto a self-primed target is a product-activated, feed-forward step that is central for the catalytic activity of Plk1 to further phosphorylate other neighboring targets in a cooperative manner (see Fig. 4*A*).

Plk1 rapidly localizes to the PBIP1-loaded kinetochores during mitosis via the function of PBD (11), raising the possibility that a PBD-dependent, two-dimensional surface interaction may occur with T78-phosphorylated PBIP1 molecules at the kinetochore plate. To investigate whether the proposed surface interaction is important for the product-activated phosphorylation of PBIPtide by Plk1, we compromised this interaction either by diluting the amount of PBIPtide immobilized on the ELISA plate or by carrying out an in vitro kinase reaction with PBIPtide in a three-dimensional solution. Dilution of PBIPtide to fivefold (0.2 μg of PBIPtide coated/well) did not alter the efficiency of PBIPtide phosphorylation, likely because of the presence of sufficient PBIPtide. However, further dilution to 20- (0.05 μg), 50- (0.02 μg), or 100-fold (0.01 μg) gradually diminished the level of the product-activated cooperativity in PBIPtide phosphorylation (Fig. 3*G*; see also Fig. S5*E*). Furthermore, Plk1 incorporated ^{32}P onto the plate-coated, two-dimensional PBIPtide much more efficiently than the in-solution, three-dimensional PBIPtide, even though the amount of PBIPtide in the former reaction was somewhat less (because of the loss of unbound PBIPtide) than that in the latter (Fig. 3*H*). These findings suggest that a sufficient amount of localized and surface-restricted PBIPtide is required for the cooperative phosphorylation of PBIPtide by Plk1. Furthermore, the amount of Plk1 recruited to the PBIP1-loaded kinetochores in Fig. 2*A* will be ultimately determined by the levels of both Plk1 activity and the surface-restricted PBIP1.

Discussion

Over the years, substantial progress has been made in identifying components crucial for targeting important regulatory proteins to a specific subcellular location. However, much less is known about the underlying mechanism of how these components interact with their binding targets and efficiently bring about particular cellular processes. In an attempt to shed light on the mechanism of one of these processes, we closely investigated the

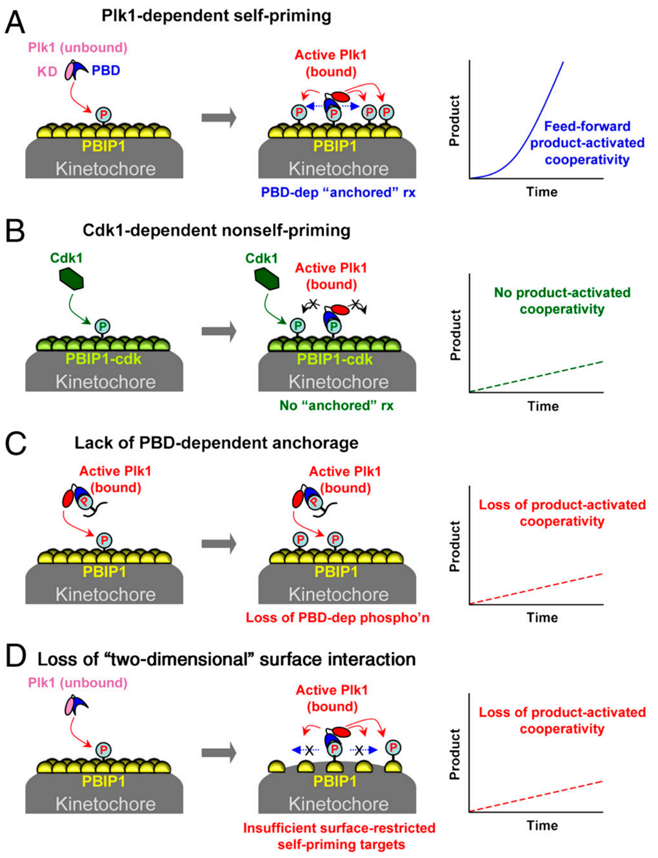

Fig. 4. Schematic drawings illustrating the modes of PBIP1 or PBIP1-cdk phosphorylation by Plk1 or Cdk1, respectively. (*A*) Unbound, partially active Plk1 phosphorylates and binds to PBIP1 at the kinetochore plate (self-priming and binding). Once anchored at the p-T78 motif of PBIP1 through its PBD, Plk1 efficiently generates multiple p-T78 epitopes on proximal PBIP1 molecules (PBD-dependent anchored reaction). These initial steps permit Plk1 to carry out two-dimensional surface interactions with neighboring p-T78-containing PBIP1 molecules (lateral dotted arrows in blue). The combination of both the PBD-dependent anchored reaction and the subsequent two-dimensional surface interactions with self-generated p-T78 motifs ensures a product-activated cooperativity in the recruitment of Plk1 to the PBIP1-loaded kinetochore plate. KD and PBD, kinase domain and PBD, respectively, of Plk1. (*B*) Cdk1 phosphorylates PBIP1-cdk and allows Plk1 to bind to the p-T78 motif of PBIP1-cdk at the kinetochore plate (non-self-priming and binding). However, bound Plk1 cannot phosphorylate neighboring PBIP1-cdk molecules (no PBD-dependent anchored reaction). In this model, the degree of T78 phosphorylation on PBIP1-cdk is linearly proportional to the level of Cdk1 activity. (*C* and *D*) Either loss of PBD-dependent binding to p-T78 PBIP1 (*C*) or absence of sufficient number of PBIP1 molecules within the kinetochore plate (*D*) prevents Plk1 from achieving a cooperative phosphorylation onto neighboring PBIP1 molecules.

biochemical basis of Plk1-dependent PBIP1 phosphorylation and its subsequent binding to kinetochore-loaded PBIP1 (11, 12). Our results demonstrate that this unusual mechanism, called self-priming and binding, is proven to be a physiologically significant process designed to achieve a cooperative formation of the Plk1–PBIP1 complex at kinetochores rather than to cope with an absence of a non-self-priming kinase, such as Cdk1, at this location. Highlighting its importance, substitution of PBIP1 with a non-self-primable PBIP1-cdk mutant led to mitotic arrest, chromosome missegregation, and apoptosis as a result of the inefficient recruitment of Plk1 to the PBIP1-loaded kinetochores.

Our data demonstrate that the generation of the p-T78 epitope on the kinetochore-bound PBIP1 is not simply the outcome of a stochastic binary interaction between Plk1 and PBIP1 in a three-dimensional environment, which should increase linearly as a function of the concentration of each component. Because the PBD-dependent interaction with the p-T78 target restricts Plk1 to the site of interaction (i.e., the kinetochore plate), the Plk1-dependent generation of the p-T78 epitope employs both three-dimensional "bulk interactions" (i.e., initial Plk1 binding to the substrates on the kinetochore plate) and subsequent two-dimensional "surface interactions" (i.e., subsequent Plk1 interactions with other substrates on the kinetochore surface without being released into solution), as described by Dennis and coworkers to explain the interaction modes of lipid-dependent enzymes (31). We propose that unbound Plk1 stochastically interacts with kinetochore-loaded PBIP1 (i.e., surface-immobilized PBIPtide in Fig. 1) and phosphorylates the latter at T78 to generate a self-binding site. Once loaded onto the kinetochore plate (i.e., the surface of the ELISA well in Fig. 1) through the interaction with its reaction product, p-T78 PBIP1, Plk1 then efficiently generates additional p-T78 epitopes on other PBIP1 molecules located proximally from the PBD-anchored site (Fig. 4*A*). Appearance of these additional p-T78 epitopes allows Plk1 to perform two-dimensional surface interactions with the former on the kinetochore plate (i.e., ELISA surface) and phosphorylate even distantly placed PBIP1 molecules with an increased efficiency (Fig. 4*A*), thus inducing a feed-forward, product-activated cooperativity. In contrast, although bound to the Cdk1-generated p-T78 motif of PBIP1-cdk, Plk1 cannot generate additional p-T78 epitopes on other PBIP1-cdk molecules, thus limiting the production of the p-T78 epitope to the level of Cdk1 availability at this location (Fig. 4*B*). Notably, lack of PBD-dependent anchorage, as a consequence of either the presence of a competitive PBD-binding phosphopeptide or the absence of a PBD-binding site on a substrate such as Hice1, completely eliminates the cooperativity in Plk1-dependent substrate phosphorylation (Fig. 4*C*). Furthermore, reactions carried out under the conditions that prevent the two-dimensional surface interaction, because of either insufficient number of surface-restricted PBIP1 molecules or lack of surface restriction onto the kinetochore plate (i.e., ELISA surface), also fail to support the cooperativity (Fig. 4*D*). These observations suggest that both the PBD-dependent anchored reaction and the two-dimensional surface interaction between Plk1 PBD and site-restricted PBIP1 are the two critical elements required for the feed-forward, product-activated cooperativity in the formation of the Plk1–PBIP1 complex.

PBD belongs to a family of phosphoepitope-binding modules that include Src-homology 2 (SH2) domain, p-Tyr-binding (PTB) domain, p-Ser/Thr/Tyr-binding protein (STYX), 14-3-3, forkhead associated (FHA) domain, and WW domain. Among these, PBD is unique in that it functions in conjunction with its *cis*-acting, N-terminal kinase domain, thus enabling Plk1 to carry out both anchored phosphorylation and two-dimensional surface interaction to achieve the cooperative formation of the Plk1–PBIP1 complex and therefore the rapid recruitment of Plk1 to mitotic kinetochores. Inactivation of Plk1 may lead to a swift reversal of this process.

Although the feed-forward control mechanism has been observed in transcriptional regulatory networks in yeast and bacteria and in metabolic network of glycolysis in the human erythrocyte (32–35), whether this mechanism operates in other intracellular events, such as mitotic processes, has not been known. This study represents a demonstration of such a mechanism that converts biochemical cooperativity into a dynamic intracellular event. Given that the number of Plk1 substrates that follow the self-priming and binding model continues to grow (10), and that most of the Plk1 substrates are restricted to surface-confined structures, such as centrosomes, kinetochores, and midbody, the observed PBD-mediated feed-forward mechanism is likely a fundamental biochemical process that ensures dynamic nature of Plk1 localization to and delocalization from multiple subcellular locations.

Materials and Methods

Construction of GST-PBIPtides. Construction of GST-PBIPtide-A_6 (hereafter referred to as GST-PBIPtide for simplicity) containing six copies of the GGPGG-fused PBIPtide fragment has been described previously (30). GST-PBIPtide-cdk_6 (hereafter referred to as GST-PBIPtide-cdk for simplicity) was generated as for the GST-PBIPtide above, except that a BamHI-BglII fragment containing PBIPtide-cdk (GGPGG-YETFDPPLHST<u>PRKR</u>DEE; the cdk mutations are underlined) was cloned into pGEX-4T-2 (Amersham Biosciences) digested with BamHI.

To generate pHR′-CMV-SV-puro-based lentiviral constructs expressing the full-length PBIP1 or PBIP1-cdk mutant, pHR′-CMV-SV-puro vector was digested with BamHI and SalI, and then ligated with a BglII-XhoI fragment of PBIP1 or PBIP1-cdk, respectively, bearing silent mutations against shPBIP1 (11). Construction of pHR′-CMV-SV-puro-FLAG-EGFP-PBIPtide or pHR′-CMV-SV-puro-FLAG-EGFP-PBIPtide-cdk was carried out by inserting a AgeI-BglII (end-filled) fragment containing either FLAG-EGFP-PBIPtide or FLAG-EGFP-PBIPtide-cdk into pHR′-CMV-SV-puro vector digested with EcoRI and end-filled.

Purification of GST-PBIPtides and GST-Hice1, ELISA-Based Kinase Reaction, and Silver Staining. Purification of GST-PBIPtide, GST-PBIPtide-cdk, and GST-Hice1 from *Escherichia coli* BL21 (DE3) was performed as described previously, using glutathione (GSH)-agarose bead (Sigma) (30). Bead-bound proteins were eluted with 100 mM GSH (pH, 8.0), and then dialyzed twice in PBS for 2 h at 4 °C.

The in vitro kinase reactions in Fig. 3*H* were carried out on a 96-well ELISA plate (Beckman Coulter, Inc.) in kinase cocktail (KC)-plus buffer [50 mM Tris-Cl (pH 7.5), 10 mM $MgCl_2$, 2 mM DTT, 2 mM EGTA, 0.5 mM Na_3VO_4, and 20 mM *p*-nitrophenyl phosphate, supplemented with 100 mM NaCl, 0.5% Nonidet P-40 and protease inhibitors] (30) in the presence of 100 μM ATP (10 μCi of [γ-^{32}P]ATP; 1 Ci = 37 GBq) and 10 ng of soluble His-Plk1 (Cell Signaling Technology) at 30 °C with gentle shaking. Either plate-coated GST-PBIPtide (for two-dimensional reaction) or in-solution GST-PBIPtide (for three-dimensional reaction) was used as substrate. To generate plate-coated GST-PBIPtide, 50 μL of soluble GST-PBIPtide (20 μg/mL in 1X ELISA coating solution) was placed in each well of the ELISA plate for 12–18 h at room temperature, and unimmobilized GST-PBIPtide was washed out before blocking with 1% BSA in PBS (see below for details). An in-solution kinase reaction was carried out immediately after the addition of soluble GST-PBIPtide. As a consequence of a low plate-coating efficiency, the amount of the plate-coated PBIPtide was significantly less than that of the in-solution PBIPtide (see Fig. 3*H*). After terminating the reactions by the addition of SDS sample buffer, the samples were separated by 10% SDS-PAGE twice, and the resulting gels were subjected either to silver staining and autoradiography or to immunoblotting analysis with anti-PBIP1 p-T78 antibody. The incorporated ^{32}P was quantified by a liquid scintillation counter.

ACKNOWLEDGMENTS. We would like to thank Paul A. Randazzo, Shilpa R. Kurian, and Susan Garfield for critical reading of the manuscript, George M. Carman for helpful discussions, and Young H. Kang and Yoshikazu Johmura for sharing the anti-CENP-Q and anti-Hice1 p-S151 antibodies, respectively. This work was supported in part by a National Cancer Institute intramural grant (K.S.L.).

1. Barr FA, Sillje HH, Nigg EA (2004) Polo-like kinases and the orchestration of cell division. *Nat Rev Mol Cell Biol* 5:429–440.
2. Archambault V, Glover DM (2009) Polo-like kinases: Conservation and divergence in their functions and regulation. *Nat Rev Mol Cell Biol* 10:265–275.
3. Petronczki M, Lénárt P, Peters JM (2008) Polo on the rise—from mitotic entry to cytokinesis with Plk1. *Dev Cell* 14:646–659.
4. van de Weerdt BC, Medema RH (2006) Polo-like kinases: A team in control of the division. *Cell Cycle* 5:853–864.
5. Jang YJ, Lin CY, Ma S, Erikson RL (2002) Functional studies on the role of the C-terminal domain of mammalian polo-like kinase. *Proc Natl Acad Sci USA* 99:1984–1989.
6. Lee KS, Grenfell TZ, Yarm FR, Erikson RL (1998) Mutation of the polo-box disrupts localization and mitotic functions of the mammalian polo kinase Plk. *Proc Natl Acad Sci USA* 95:9301–9306.
7. Seong YS, et al. (2002) A spindle checkpoint arrest and a cytokinesis failure by the dominant-negative polo-box domain of Plk1 in U-2 OS cells. *J Biol Chem* 277:32282–32293.
8. Cheng KY, Lowe ED, Sinclair J, Nigg EA, Johnson LN (2003) The crystal structure of the human polo-like kinase-1 polo box domain and its phospho-peptide complex. *EMBO J* 22:5757–5768.
9. Elia AE, et al. (2003) The molecular basis for phospho-dependent substrate targeting and regulation of Plks by the polo-box domain. *Cell* 115:83–95.
10. Park JE, et al. (2010) Polo-box domain: A versatile mediator of polo-like kinase function. *Cell Mol Life Sci* 67:1957–1970.
11. Kang YH, et al. (2006) Self-regulation of Plk1 recruitment to the kinetochores is critical for chromosome congression and spindle checkpoint signaling. *Mol Cell* 24:409–422.
12. Lee KS, et al. (2008) Mechanisms of mammalian polo-like kinase 1 (Plk1) localization: Self- versus non-self-priming. *Cell Cycle* 7:141–145.
13. Minoshima Y, et al. (2005) The constitutive centromere component CENP-50 is required for recovery from spindle damage. *Mol Cell Biol* 25:10315–10328.
14. Foltz DR, et al. (2006) The human CENP-A centromeric nucleosome-associated complex. *Nat Cell Biol* 8:458–469.
15. Okada M, et al. (2006) The CENP-H-I complex is required for the efficient incorporation of newly synthesized CENP-A into centromeres. *Nat Cell Biol* 8:446–457.
16. Neef R, et al. (2007) Choice of Plk1 docking partners during mitosis and cytokinesis is controlled by the activation state of Cdk1. *Nat Cell Biol* 9:436–444.
17. Burkard ME, et al. (2009) Plk1 self-organization and priming phosphorylation of HsCYK-4 at the spindle midzone regulate the onset of division in human cells. *PLoS Biol* 7 e1000111.
18. Neef R, et al. (2003) Phosphorylation of mitotic kinesin-like protein 2 by polo-like kinase 1 is required for cytokinesis. *J Cell Biol* 162:863–875.
19. Wysocka J, Liu Y, Kobayashi R, Herr W (2001) Developmental and cell-cycle regulation of Caenorhabditis elegans HCF phosphorylation. *Biochemistry* 40:5786–5794.
20. Holmes JK, Solomon MJ (1996) A predictive scale for evaluating cyclin-dependent kinase substrates. A comparison of p34cdc2 and p33cdk2. *J Biol Chem* 271:25240–25246.
21. Lenart P, et al. (2007) The small-molecule inhibitor BI 2536 reveals novel insights into mitotic roles of polo-like kinase 1. *Curr Biol* 17:304–315.
22. Seong YS, et al. (2003) Characterization of a novel cyclin-dependent kinase 1 inhibitor, BMI-1026. *Cancer Res* 63:7384–7391.
23. Golsteyn RM, Mundt KE, Fry AM, Nigg EA (1995) Cell cycle regulation of the activity and subcellular localization of Plk1, a human protein kinase implicated in mitotic spindle function. *J Cell Biol* 129:1617–1628.
24. Lee KS, Yuan YL, Kuriyama R, Erikson RL (1995) Plk is an M-phase-specific protein kinase and interacts with a kinesin-like protein, CHO1/MKLP-1. *Mol Cell Biol* 15:7143–7151.
25. Elowe S, Hümmer S, Uldschmid A, Li X, Nigg EA (2007) Tension-sensitive Plk1 phosphorylation on BubR1 regulates the stability of kinetochore microtubule interactions. *Genes Dev* 21:2205–2219.
26. Qi W, Tang Z, Yu H (2006) Phosphorylation- and polo-box-dependent binding of Plk1 to Bub1 is required for the kinetochore localization of Plk1. *Mol Biol Cell* 17:3705–3716.
27. Goto H, et al. (2006) Complex formation of Plk1 and INCENP required for metaphase-anaphase transition. *Nat Cell Biol* 8:180–187.
28. Ahonen LJ, et al. (2005) Polo-like kinase 1 creates the tension-sensing 3F3/2 phosphoepitope and modulates the association of spindle-checkpoint proteins at kinetochores. *Curr Biol* 15:1078–1089.
29. Chen Q, Zhang X, Jiang Q, Clarke PR, Zhang C (2008) Cyclin B1 is localized to unattached kinetochores and contributes to efficient microtubule attachment and proper chromosome alignment during mitosis. *Cell Res* 18:268–280.
30. Park JE, et al. (2009) Direct quantification of polo-like kinase 1 activity in cells and tissues using a highly sensitive and specific ELISA assay. *Proc Natl Acad Sci USA* 106:1725–1730.
31. Carman GM, Deems RA, Dennis EA (1995) Lipid signaling enzymes and surface dilution kinetics. *J Biol Chem* 270:18711–18714.
32. Bali M, Thomas SR (2001) A modelling study of feedforward activation in human erythrocyte glycolysis. *Proceedings of the Academy of Sciences, Series III*, (Life Sciences, Paris), 324, pp 185–199.
33. Hayot F, Jayaprakash C (2005) A feedforward loop motif in transcriptional regulation: Induction and repression. *J Theor Biol* 234:133–143.
34. Ratushny AV, et al. (2008) Control of transcriptional variability by overlapping feed-forward regulatory motifs. *Biophys J* 95:3715–3723.
35. Mangan S, Alon U (2003) Structure and function of the feed-forward loop network motif. *Proc Natl Acad Sci USA* 100:11980–11985.